ACADEMIC PRESS

Available online at www.sciencedirect.com
SCIENCE DIRECT®

Journal of Catalysis 217 (2003) 310–323

JOURNAL OF CATALYSIS

www.elsevier.com/locate/jcat

Nature and catalytic role of active silver species in the lean NO_x reduction with C_3H_6 in the presence of water

A. Iglesias-Juez,[a] A.B. Hungría,[a] A. Martínez-Arias,[a] A. Fuerte,[a] M. Fernández-García,[a,*] J.A. Anderson,[b] J.C. Conesa,[a] and J. Soria [a]

[a] *Instituto de Catálisis y Petroleoquímica, CSIC, Campus Cantoblanco, 28049 Madrid, Spain*
[b] *Division of Physical and Inorganic Chemistry, University of Dundee, Dundee DD1 4HN, Scotland, UK*

Received 24 September 2002; revised 23 January 2003; accepted 3 February 2003

Abstract

A study of the lean NO_x reduction activity with propene in the presence of water over Ag/Al_2O_3 catalysts with different silver loadings (1.5–6 wt%) has been done using X-ray diffraction, ultraviolet–visible spectroscopy, transmission electron microscopy, and in situ diffuse reflectance infrared and X-ray absorption spectroscopies under reaction conditions. The catalysts were prepared by an impregnation method employing EDTA complexes that allow highly dispersed silver phases to be obtained, which are stabilized under reaction conditions by strong interactions with the support. It is shown that the active species corresponds to silver aluminate-like phases with tetrahedral local symmetry. The role of silver in the reaction mechanism is shown to be mainly in the activation of NO_x and propene species. In particular, the silver entities have been found to offer a new reaction path for propene activation which involves generation of acrylate species as a partially oxidized active intermediate. Differences between two active catalysts containing 1.5 and 4.5 wt% of Ag suggest that optimization of the SCR activity can be related to the oxygen lability of the tetrahedral silver aluminate-like phase present in the catalyst. As postulated previously, the high nonselective propene oxidation activity of the highest loaded sample (with 6 wt% Ag) appears to be related to formation of metallic silver surface states at low reaction temperatures which are active for NO dissociation.

Keywords: NO_x-propene SCR; Ag/Al_2O_3 catalysts; In situ DRIFTS; XAFS; UV–vis; XRD; TEM

1. Introduction

Selective catalytic reduction (SCR) of NO_x in the oxygen-rich exhaust streams of lean-burn engines remains one of the major challenges for environmental catalysis. Cu-ZSM-5 was the first catalyst displaying good lean NO_x reduction activity [1]; however, zeolite-based systems lack stability in the presence of water or sulfur dioxide [2]. The best results in this respect have been observed when using alumina-supported systems [3–5]. Among these, Pt and Pd catalysts have shown high activity for the reaction, presenting NO_x conversion windows at much lower temperatures than zeolite-based catalysts [6]. They are, however, highly selective toward N_2O, an undesirable greenhouse gas [7]. Alumina-supported nonnoble metal oxide systems (among others, those of tin, cobalt, and silver) are effective catalysts, although at a higher temperature window than noble metal systems, for the lean NO reduction with C_3H_6 in the presence of water and all of these apparently operate through a very similar reaction mechanism [4,8,9]. The catalytic activity of these materials is maintained at a relatively high level even in the presence of H_2O and SO_2 [8,10–13]. Higher NO conversions at lower temperatures are generally observed when using oxygenated hydrocarbons, such as ethanol and acetone, as reductants instead of propene [8]. Unfortunately, harmful by-products, such as hydrogen cyanide, can be formed when using such reductants [14].

The effectiveness of the Ag/Al_2O_3 catalyst depends greatly on the Ag loading, the best catalytic performance being achieved with intermediate loadings (2–3%, for systems employing typical high surface area γ-Al_2O_3 materials as support) [8,15–18]. Higher silver loadings produce higher rates of C_3H_6 oxidation with O_2, at the expense of its reaction with NO. This has been attributed to the detrimental effect of increasing the particle size of silver oxide

* Corresponding author.
E-mail address: m.fernandez@icp.csic.es (M. Fernández-García).

0021-9517/03/$ – see front matter
doi:10.1016/S0021-9517(03)00055-1

species, yielding reducible entities (leading to Ag^0) more readily with a higher activity for nonselective propene oxidation [15–18]. It has been proposed that for size-limited clusters, silver can be stabilized in an oxidized (Ag^+) state, as a consequence of the interaction with the alumina support, which would constitute the active centers for the NO_x reduction reaction [15]. This theory, however, has recently been challenged [17]. In this respect, an Ag/Al_2O_3 catalyst has been reported to show markedly improved performance after an XRD-detectable silver aluminate phase was generated by hydrothermal treatment at 1073 K [19]. The presence of silver aluminates has also been reported as part of the active metal chemical distribution in other alumina-supported samples [17,19]. It may also be recalled that, when present as exchanged cations in zeolites, i.e., a situation where large particles of oxide or metal are less readily formed, NO_x conversion (using CH_4 as reductant) does not decrease with Ag loading below ca. 10 wt% [5,20].

The aim of the present work is to study the catalytic activity for lean NO reduction with C_3H_6 in the presence of water over Ag/Al_2O_3 catalysts prepared by an impregnation method designed to maximize the amount of active silver phases. Emphasis will be placed on the structural analysis of the silver phases of most active samples. For these purposes, a multi-technique approach has been followed using X-ray diffraction (XRD), transmission electron microscopy (TEM), UV–vis spectroscopy for catalyst characterization, and employing in situ diffuse reflectance infrared Fourier transform (DRIFTS), and X-ray absorption spectroscopies (XAFS) to gain insight into the redox and chemical changes occurring during the course of the reaction as well to gain key information concerning the activation of reactant molecules and the interaction with adsorbed species.

2. Experimental

Alumina-supported silver catalysts of different Ag loadings were prepared using $AgNO_3$ (supplied by Aldrich) as silver precursor and Al_2O_3 (Condea, $S_{BET} = 200\ m^2\,g^{-1}$) as support. Aqueous solutions containing different $AgNO_3$ concentrations (in order to obtain final nominal silver loadings of 1.5, 4.5, and 6 wt%) were first mixed with EDTA in 1:2.2 molar ratio (aiming to produce negatively charged silver complexes, which may interact with the positively charged surface alumina at pH about 6.3—obtained by using tetramethylammonium hydroxide (TMAH) as base of the buffer system) and subsequently used to impregnate the alumina support by the incipient wetness technique. The solids were then dried for a short period at room temperature and then at 383 K for 24 h and finally calcined in air at 773 K for 2 h. Ag analyses of the samples by ICP-AES yielded values which coincide, within the error limits, with the nominal values. Samples are denoted as 1.5Ag, 4.5Ag, and 6Ag, in accordance with the weight loadings. BET surface areas showed values similar to that of the parent alumina for all the samples.

Powder XRD patterns were recorded on a Siemens D-500 diffractometer using nickel-filtered Cu-K_α radiation operating at 40 kV and 25 mA and with a 0.02° step size. Samples for transmission electron microscopy were prepared by crushing in an agate mortar, dispersing in isobutanol, and depositing on perforated carbon films supported on copper grids. TEM data were obtained on a JEOL 2000 FX II system (with 3.1 Å point resolution) equipped with a LINK probe for energy-dispersive analysis (EDX). Around 10 aggregates and 2 to 4 zones per aggregate were analyzed for each sample. A Varian UV–vis spectrophotometer, Model 2300, was used for the recording UV–vis absorption spectra (transmittance) of bulk samples of squared shape and 0.5 cm of path length.

Catalytic activity tests were performed in a Pyrex flow reactor system using a feed stream consisting of 0.1% NO, 0.1% C_3H_6, 5% O_2, and 3% H_2O (N_2 balance; ca. $1 \times 10^3\ cm^3\,min^{-1}\,g^{-1}$ at a fix space velocity of $4 \times 10^4\ h^{-1}$). The effluent from the reactor, with the exception of H_2O which was (mostly) removed by a cold trap (NaCl–ice mixture), was analyzed on line using a Perkin-Elmer 1725X FTIR spectrometer coupled with a multiple reflection transmission cell (Infrared Analysis Inc.). In all cases the samples were subjected to an in situ calcination pretreatment under dry air at 773 K. Typical tests were performed in the light-off mode by increasing the temperature at $5\ K\,min^{-1}$ from 298 to 823 K.

In situ DRIFTS experiments were performed using a Perkin-Elmer 1750 FTIR fitted with an MCT detector. The DRIFTS cell (Harrick) was equipped with CaF_2 windows and a heating cartridge that allowed samples to be heated up to 773 K. The spectral resolution employed was $4\ cm^{-1}$. Samples of ca. 80 mg were calcined in situ in dry air at 773 K. The spectra were taken by accumulating 25 scans, except where noted otherwise. The composition of the inlet gases was manipulated by a computer-controlled gas blender with $80\ cm^3\,min^{-1}$ passing through the catalyst bed, and with the NO_x gases in the outlet from the DRIFTS cell monitored by a chemiluminiscence analyzer (Thermo Environmental Instruments 42C).

In situ X-ray absorption experiments at the Ag K-edge were performed at the BM29 line of the ESRF synchrotron at Grenoble. A Si(111) monochromator, detuned at 50% to minimize harmonic content of the beam, and ionization chambers filled with Kr/Ar were used to obtain the transmission XAFS data. An Ag foil between the second and a third ionization chamber was measured simultaneously to calibrate the energy scale. Self-supported wafers (absorbance below 0.5) were placed in a controlled-atmosphere cell for treatment under controlled atmosphere and temperature. EXAFS spectra were obtained using standard procedures; preedge substraction was performed by using a Victoreen formula, postedge substraction using a cubic spline procedure, and normalization by fixing to one the value of a

postedge background point at about 50 eV from the edge. Phase and amplitude functions from the Ag_2O reference EXAFS spectra were used to analyze Ag–O contributions in used and freshly calcined Ag samples. Analysis of EXAFS signals was performed over a K range from 1.95 to 8.2 $Å^{-1}$ and an R range from 0.7 to 3.22 Å. This implies a number of free parameters, according to the Nyquist theorem, of 12 [21].

3. Results

3.1. Catalytic activity tests

Fig. 1 shows the propene (A) and NO_x ($NO + NO_2$) to N_2 (B) conversions, along with the yields of CO (C), NO_2 (D), and N_2O (E) for the C_3H_6-SCR of NO in the presence of water. No carbon-containing products other than CO_2 and

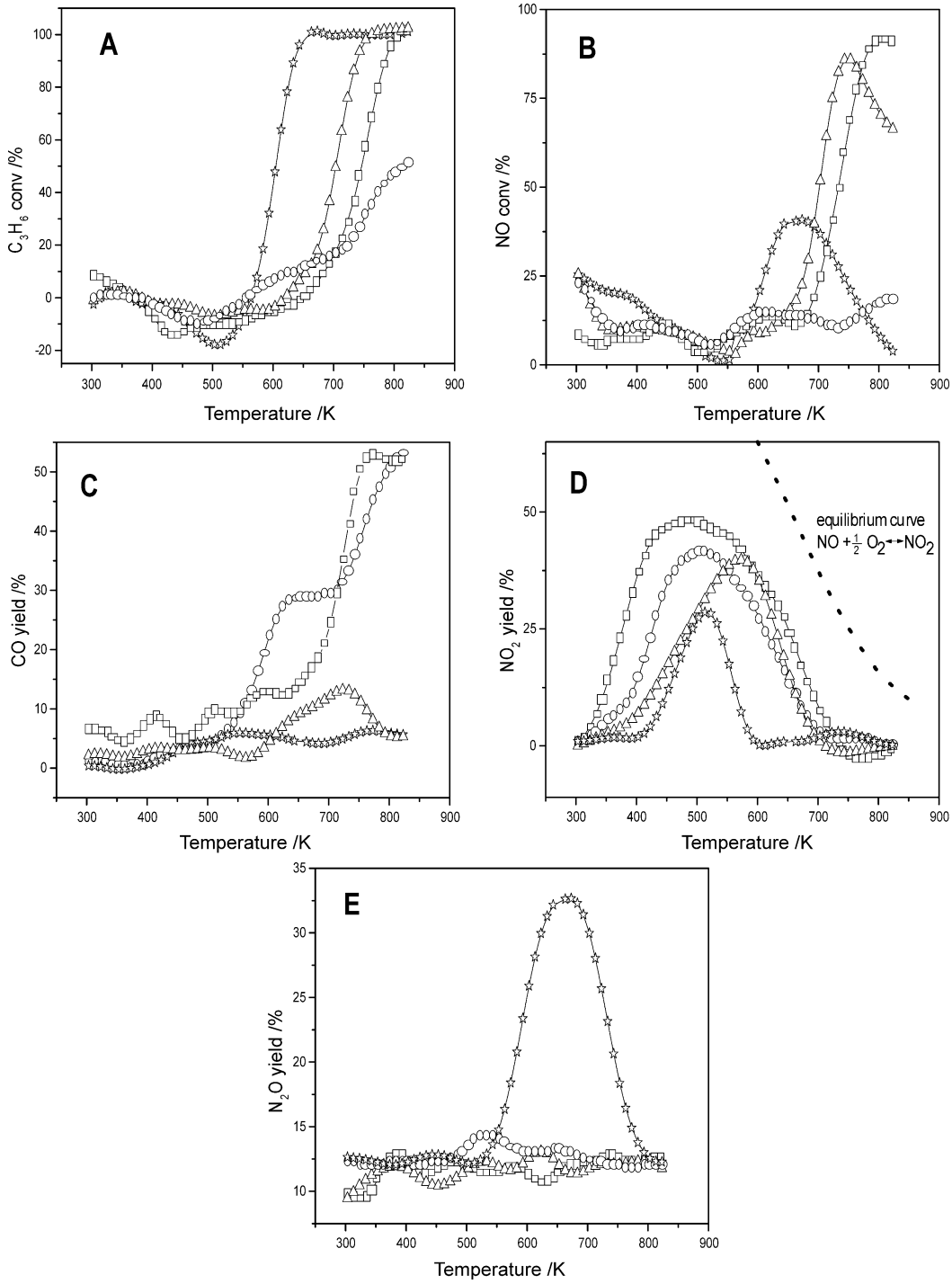

Fig. 1. Conversion of propene (A) and NO_x (B) to nitrogen for Ag samples and alumina support. Yields to CO (C), NO_2 (D), and N_2O (E) are also displayed. Circles, alumina; squares, 1.5Ag; triangles, 4.5Ag; stars, 6Ag.

CO (e.g., oxygenated hydrocarbons) were detected in the evolved gases, with a marked trend to decrease selectivity to the latter product with increasing the Ag content of the catalyst. NO, on the other hand, was partially converted to NO_2 at low temperatures (where absence of propene conversion can be noted), mostly through the homogeneous reaction with oxygen (Fig. 1D). Parallel to hydrocarbon conversion, NO reduction products are detected; because N_2O production is modest (Fig. 1E) and no other N-containing molecule (e.g., NH_3) is detected, it can be said that NO_x were essentially converted to N_2 in all cases except for 6Ag. The alumina support showed low SCR activity, which can be attributed to deactivation of the system induced by the presence of water [8], a fact never observed in Ag-containing systems (see Ref. [18] and references therein). Certain differences in terms of catalytic performance were noted between these catalysts and other Ag/Al_2O_3 systems reported in the literature. Thus, CO selectivity has not been typically reported for catalysts prepared by impregnation with aqueous silver nitrate solutions [7,22] while C_3H_6 conversion levels are generally higher here than those achieved in our laboratory with catalysts prepared by a microemulsion method [18]. Production of significant amounts of carbon monoxide, here detected for the alumina carrier and the 1.5Ag sample, appears to be a characteristic of acidic catalysts [23]. Comparison of the NO_x reduction activity of these samples reveals only subtle differences at $T < 600$ K at which low NO_x conversions are observed; in view of the absence of C_3H_6 oxidation under these conditions, the NO_x consumption can be mostly attributed to adsorption phenomena.

The results indicate the promoting effect of silver at intermediate loadings on the SCR reaction, in agreement with previous reports [8,15–18]. Thus, the 1.5Ag and 4.5Ag samples are active for NO_x reduction, showing similar NO_x and C_3H_6 conversion profiles but shifted to lower temperatures for the 4.5Ag. On the other hand, the catalytic behavior of the sample with the highest silver loading (6Ag) shows similarities with previous studies [7,16,18, 22], indicating that low NO_x conversion levels are achieved over alumina-supported samples with relatively high silver loadings, while a relatively higher rate for the nonselective C_3H_6 combustion occurs.

3.2. Sample characterization

Samples in their calcined state were analyzed by several techniques. ED and XRD data (not shown) of calcined and postreaction samples only displayed alumina-related features without significant differences between samples. Only a limited number of amorphous (i.e., not detected by diffraction techniques) Ag particles were visible in some TEM micrographs. However, the number of silver particles detected during sampling was very small compared with previous experience of silver–alumina systems [17,18], a fact that will be discussed below in light of XAFS results.

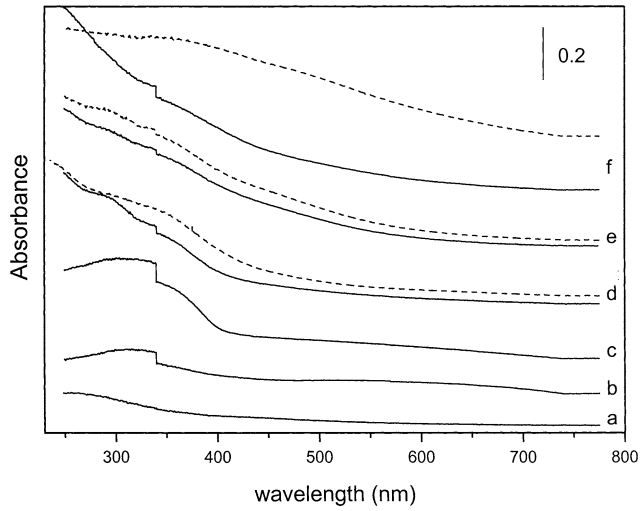

Fig. 2. UV–vis spectra of Ag samples and reference compounds: (a) α-$AgAlO_2$, (b) Ag_2O, (c) β-$AgAlO_2$, (d) 1.5Ag, (e) 4.5Ag, and (f) 6Ag. Full line, calcined materials; dashed line, postreaction materials.

UV–vis spectra of calcined and postreaction samples and reference compounds are shown in Fig. 2. Only minor differences were noted among calcined samples indicating the similar nature of the initial, supported silver species; larger differences were, however, encountered between the 6Ag sample and the others after reaction. In the latter case, a broad band centered at ca. 350 nm was detected, which can be attributed to the presence of small Ag(0) clusters [16,17]. This indicates a reasonable degree of stability of the Ag phase in the 1.5Ag and 4.5Ag samples and the evolution under reaction conditions for the 6Ag to yield metallic silver particles.

DRIFT spectra of the alumina and fresh 1.5Ag, 4.5Ag, and 6Ag samples calcined in dry air at 773 K are shown in Fig. 3. The samples show similarities in the hydroxyl stretching region with bands at 3754, 3720, 3678, and 3631 cm^{-1},

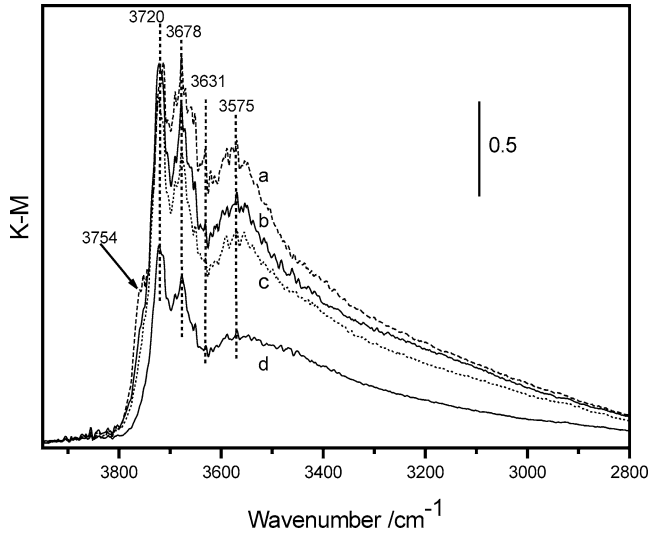

Fig. 3. IR spectra corresponding to the OH stretching region for samples in their calcined state: (a) alumina, (b) 1.5Ag, (c) 4.5Ag, and (d) 6Ag.

and a broader one below 3600 cm^{-1} showing a maximum around 3575 cm^{-1}. These bands can all be attributed to diverse surface Al–OH groups. Bands in the 3800–3600 cm^{-1} region correspond to different isolated hydroxyl species, their frequency being related to the nature of the Al cation and/or to the coordination number of the corresponding hydroxyl group [24]. On the other hand, the broad band peaking at 3575 cm^{-1} can be assigned to associated (mutually interacting by hydrogen bonds) hydroxyl groups [23]. Decreased intensity was detected upon increasing the amount of silver deposited on alumina, which mainly affected the most basic (3754 cm^{-1}) and acidic (3631 and 3575 cm^{-1}) hydroxyls for the 1.5Ag sample and progressively decreased the intensity of the remaining terminal OH groups, with particular effect in the 6Ag case. It was noted, however, that a general decrease in intensity for the 6Ag spectrum occurred over the whole 3800–2800 cm^{-1} region, Fig. 3, suggesting that the reflectance from the solid was different from the other samples. However, by analyzing the 1250–1000 cm^{-1} region (result not shown), characteristic of alumina skeletal vibrations and the OH deformation modes (1000–1050 cm^{-1}), we can conclude that a change in surface hydration of the samples does contribute to the (OH region) intensity behavior noted.

3.3. *In situ DRIFTS experiments*

In order to identify the different species formed by chemisorption of the different reactants, which might allow a degree of rationalization in terms of the catalytic behavior of these systems, a series of infrared experiments were performed by subjecting the samples to specific reactant mixtures starting with simple mixtures and gradually introducing the other reactant components. Following calcination in dry air at 773 K, the samples were cooled under the dry air flow to temperatures ranging from 573 to 723 K (see below) before switching to inert gas (N_2) for 15 min and recording a background spectrum under these conditions. The desired reactant gases (diluted in N_2) were then introduced at a fixed temperature (leaving 15–45 min contact with the corresponding reactant gases before recording the spectrum in each case, ensuring the stability of band intensity) and the changes in the infrared spectra recorded (100 scans being accumulated for these experiments). Different recording temperatures, calculated to attain conversions of NO_x (Fig. 4) and C_3H_6 (Fig. 5) of about 20% with the full mixture, are included in these figures. These are intended to provide a representative (though approximate) picture of the surface species which might be involved in the reaction mechanism.

Introduction of NO alone induced only minor changes in the IR spectra (Figs. 4Aa–Da), whereas more drastic changes occurred when a $NO + O_2$ mixture was allowed to contact the sample (Figs. 4Ab–Db). The latter treatment led to the appearance of two groups of bands in the spectra of the alumina and supported Ag samples (Figs. 4Ab–Db) at ca. 1550 and 1245 cm^{-1} (type I) and 1580–1560 and 1305 cm^{-1} (type II), that can be attributed to different (monodentate and/or bidentate) nitrate species adsorbed on the alumina surface [18,22,25,26]. In the case of 6Ag, bulk-like nitrite (NO_2^-) species giving a band at 1300 cm^{-1} [22] might also be formed (Fig. 6Da,b). Similar adsorbed NO_x species have previously been observed for Ag/Al_2O_3 [18,22,25,27]. Small differences between catalysts regarding band frequencies for nitrate species can be ascribed to slight differences in the local environment of adsorption sites. Certain differences were additionally observed between the alumina and the silver-containing samples concerning involvement of hydroxyl species during nitrate formation

$$OH(ad) + NO_2(g) \rightarrow HNO_3(ad) \leftrightarrow H^+(ad) + NO_3^-.$$

Thus, while a net consumption of acidic hydroxyls (bands at 3632 and 3542 cm^{-1}) was apparent for the silver-free alumina, the hydroxyl species were less perturbed during nitrate formation for the silver-containing samples.

Clearer differences due to the presence of silver were observed in the presence of species formed upon partial oxidation of the hydrocarbon, as detected following subsequent addition of C_3H_6 to the flowing gas mixture (Figs. 4Ac,d to 4Dc,d). Thus, while a group of bands at ca. 1642, $\approx$ 1575, 1454–1458, 1378–1392, and 1296–1298 cm^{-1}, attributed to vibrations of adsorbed acrylate species [18,22,25,28], were observed for Ag-containing samples, no acrylate was apparent for the alumina sample, in which case propene oxidation appeared to proceed mainly to formate species (bands at 3000, 2907, 1589, 1392, and 1375 cm^{-1}), probably via interaction of CO or, less likely, of CO_2 with the alumina surface. Additionally, a further carboxylate-type species (giving rise to bands at ca. 1540 and 1455 cm^{-1}) [25,26] was observed for all the samples. It can be noted that bicarbonate ad-species, formed from CO_2, can contribute to the spectra with bands at 1648, 1453, and 1230 cm^{-1}; however, absence of intensity at 3605 cm^{-1} eliminates such possibility. In general terms, introduction of propene to the reaction mixture induced concomitant decreases or complete disappearance of nitrate groups, particularly those of type II. Changes were noted in the hydroxyl stretching region upon introduction of propene, which mainly involved a depletion of the more basic hydroxyl species (at 3769–3747 cm^{-1}) and generation of acidic hydroxyls (at 3567–3542 cm^{-1}). In general terms, a net production of hydroxyl species was apparent following exposure of the NO_x covered surface to propene, except for the 6Ag sample which showed significantly greater consumption of basic hydroxyls during the process.

For the 1.5Ag and 4.5Ag systems, experiments performed by introducing the samples initially to a $C_3H_6 + O_2$ mixture (Figs. 5A and 5B) confirm the formation of acrylate species (bands at 1642–1643, 1572–1575, 1456–1461, 1383–1372, and $\approx$ 1300 cm^{-1}) and in addition, the presence of the other carboxylate-type species (bands at ca. 1540 and 1460–1455 cm^{-1}). The concentration of surface acrylate increased following the subsequent addition of NO, which in turn led to the generation of nitrate species for the 4.5Ag sample.

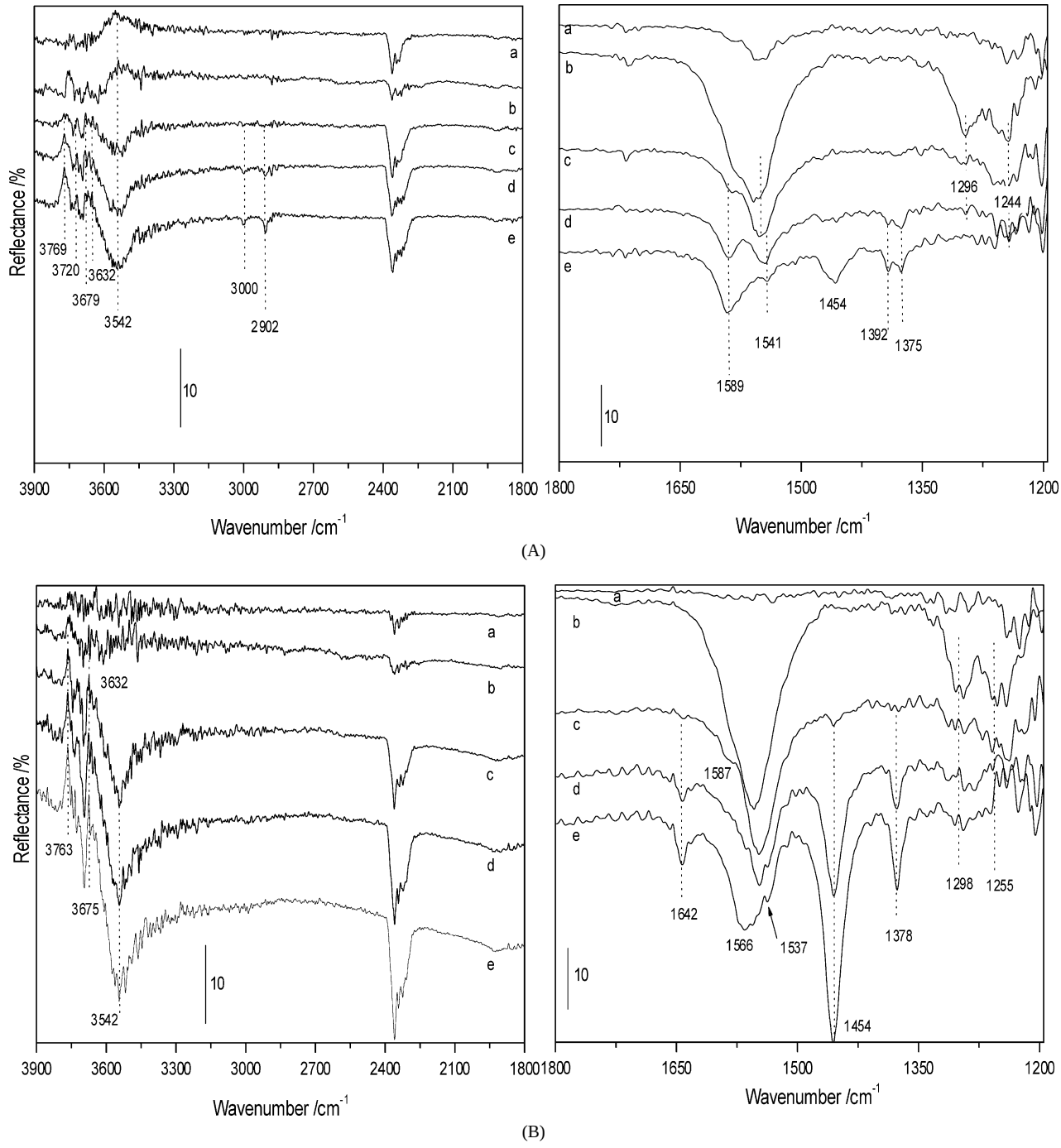

Fig. 4. DRIFTS spectra at temperatures corresponding to 20% NO conversion for (A) alumina, (B) 1.5Ag, (C) 4.5Ag, and (D) 6Ag after consecutive treatment with 1800 ppm of NO (a), and subsequent addition of 5% O_2 (b), 900 ppm of propene (c), and up to 1800 ppm of propene (d). Complete gas mixture after 1 h (e).

Hydroxyl groups evolved in a similar way as described in the former paragraph; thus, contact with the C_3H_6–O_2 mixture generated acidic hydroxyls (3553 cm^{-1}) while the more basic ones (3770–3760, 3725, and 3680–3660 cm^{-1}) were consumed. As in the experiments of Fig. 4, analysis of the overall intensity suggests that a net formation of hydroxyl species was already produced during propene oxidation with oxygen. Of course, formation of water during the experiment may also contribute to reduce intensity of "isolated" hydroxyls and enhance that of associated groups.

DRIFT spectra of the samples recorded under reaction conditions at increasing temperatures are shown in Figs. 6A–D. Analysis of these results essentially confirms the points noted for experiments performed using sequential admission of adsorbates (Figs. 4 and 5). Thus, for the alu-

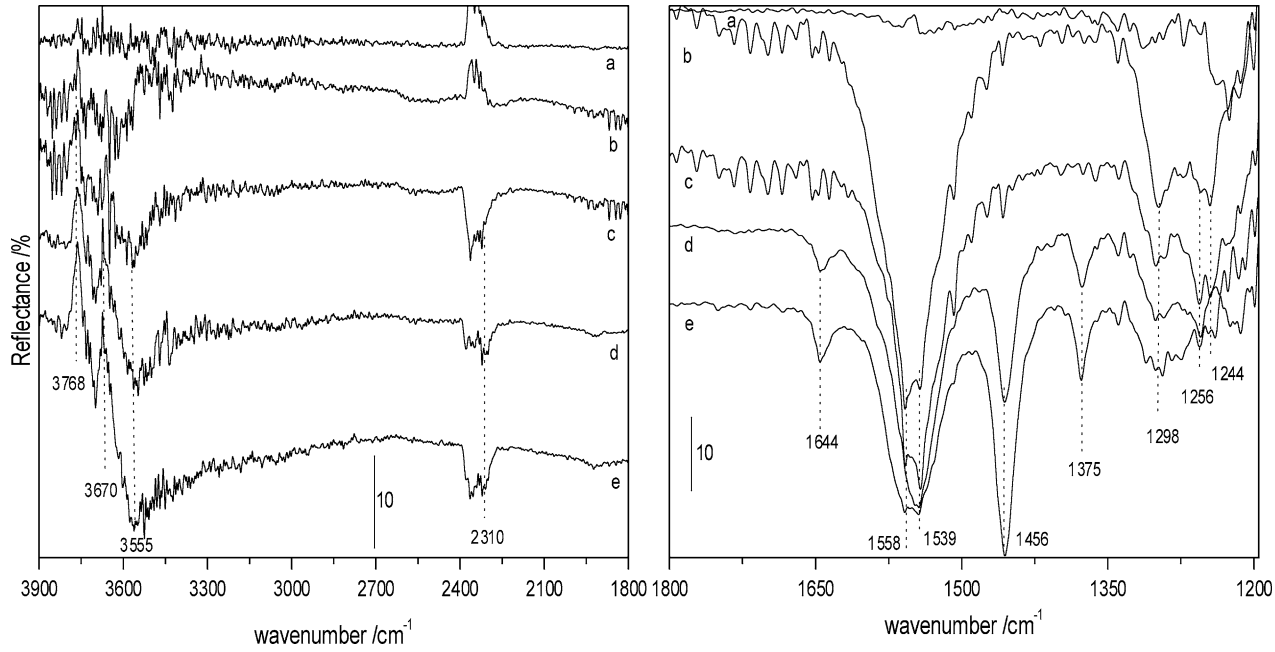

(C)

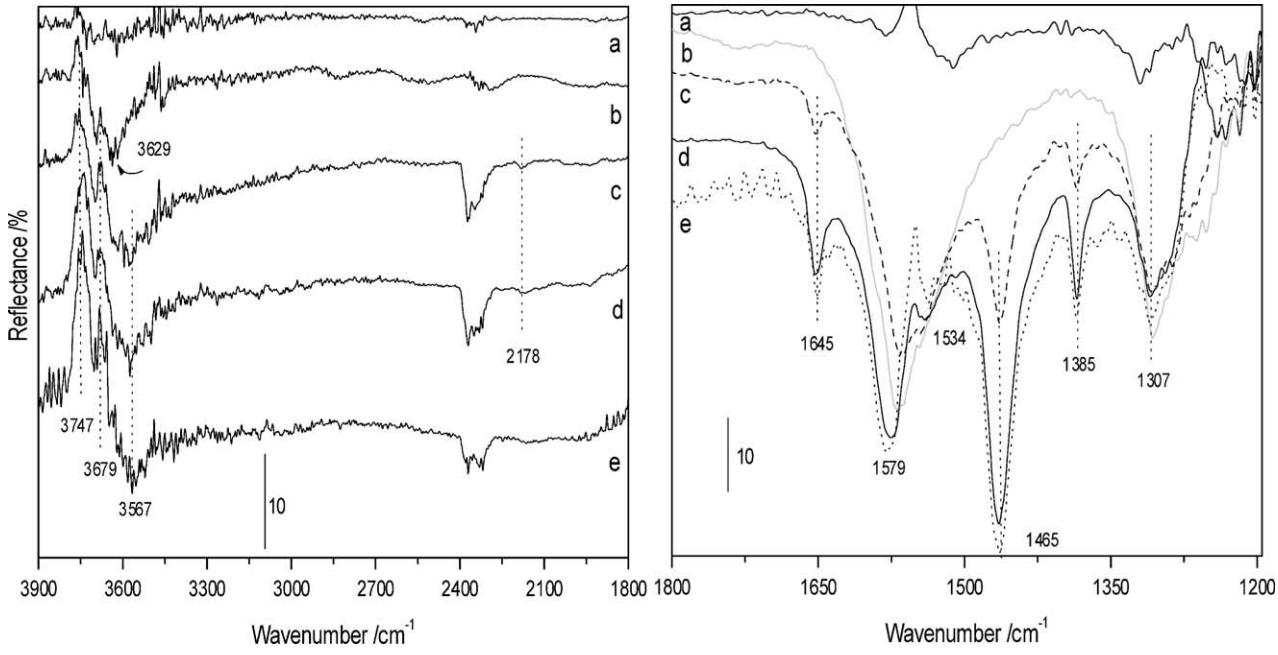

(D)

Fig. 4. Continued.

mina alone, (Figs. 6A), propene oxidation appears to lead to the formation of adsorbed formate species (bands at 3000, 2907, 1590, 1391, and 1376 cm^{-1}), and, likely, of a higher carbon carboxylate-type compound (evidenced by the presence of the band at 1460 cm^{-1}). In contrast, acrylate species were somewhat detected for the active silver-containing (1.5Ag and 4.5Ag) samples, as characterized by the detection of the weak bands at $\approx$ 1645, 1580, and 1390 cm^{-1}. In general terms, the temperature at which maximum intensity of bands due to carboxylate-type species was observed (according to the intensity of the band at 1460–1455 cm^{-1}) decreased with increasing silver loading, which is also in accordance with the evolution of the CO_2 gas contribution (bands at 2400–2200 cm^{-1}), which, in turn, roughly follows the propene conversion profiles obtained during the catalytic tests (Fig. 1A). Other effects induced by the presence of silver concern the formation of mono- and/or bidentate nitrates (1585–1590 and 1305 cm^{-1}, and 1545–1550, and 1250 cm^{-1}) and bridging nitrates or adsorbed NO_2 (1611–1616 cm^{-1}) [18,22,25,28,29] immediately following

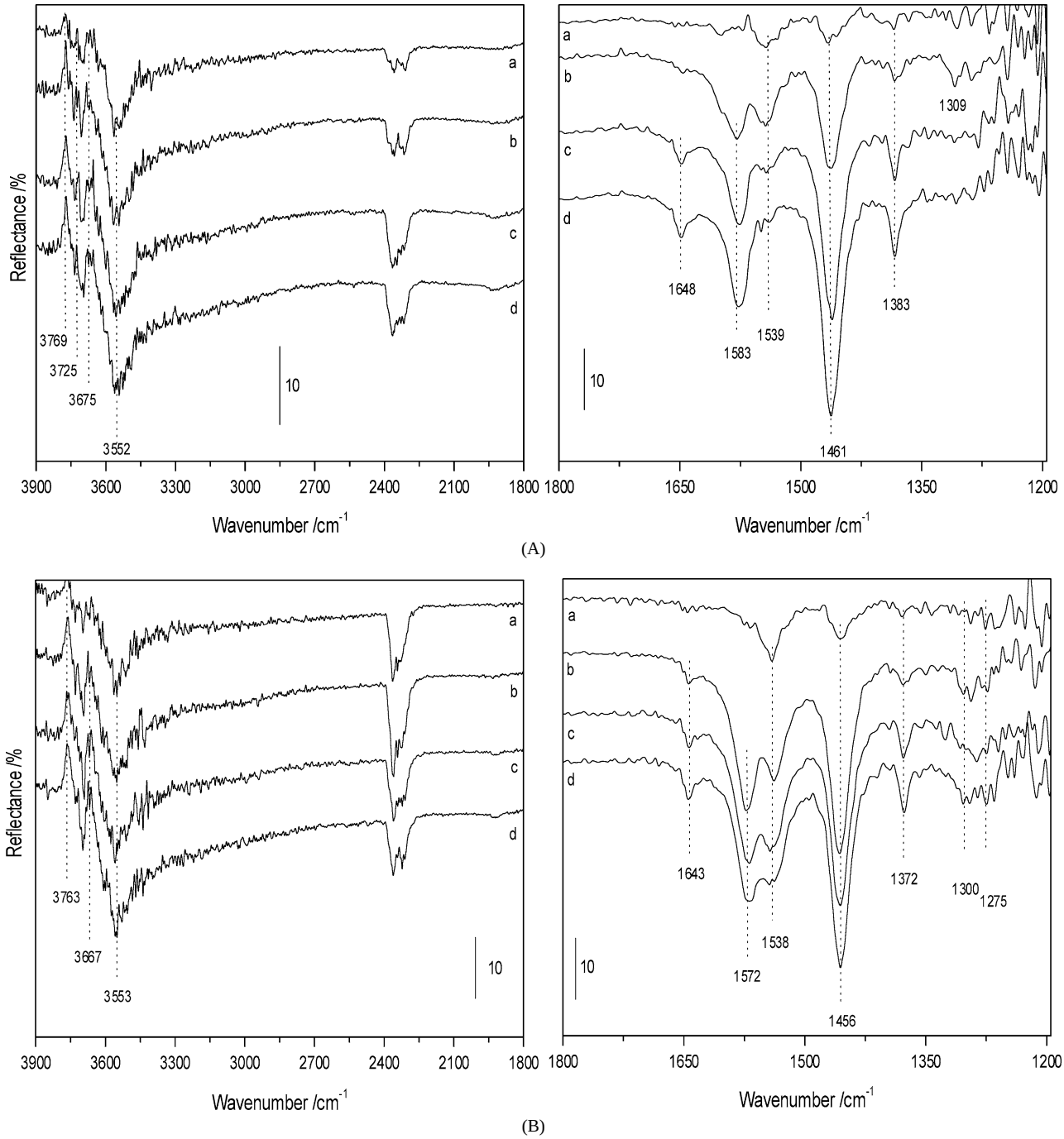

Fig. 5. DRIFTS spectra at temperatures corresponding to 20% propene conversion for (A) 1.5Ag, and (B) 4.5Ag, after consecutive treatment with 900 ppm of propene +5% O_2 (a), and subsequent addition up to 1800 ppm of propene (b), 900 ppm of NO (c), and up to 1800 ppm of NO (d).

exposure to the reactive mixture. These species rapidly depleted on raising the temperature, particularly those giving bands at ca. 1590 and 1305 cm^{-1} (type II nitrate). In general, a small amount of the type I nitrate (bands at ca. 1550 and 1250 cm^{-1}) was retained even at the highest sample temperature. A significant difference between sample 6Ag and the other two silver-containing samples (or the alumina alone) was the identification of cyanide species (band at 2170 cm^{-1}—Fig. 6) for the former, appearing initially at 573 K. This appears to be a particular characteristic of this sample as indicated by the detection of a small amount of such cyanide species upon introduction of C_3H_6 in the experiments of Fig. 4D. The absence of type II nitrates was also noticeable. These points taken together suggest that a distinct pathway for NO dissociation/activation exists over sample 6Ag. Other features appearing in the spectra under reaction conditions (Fig. 6) include those giving a broad band between 2311 and 2237 cm^{-1}. These bands are prob-

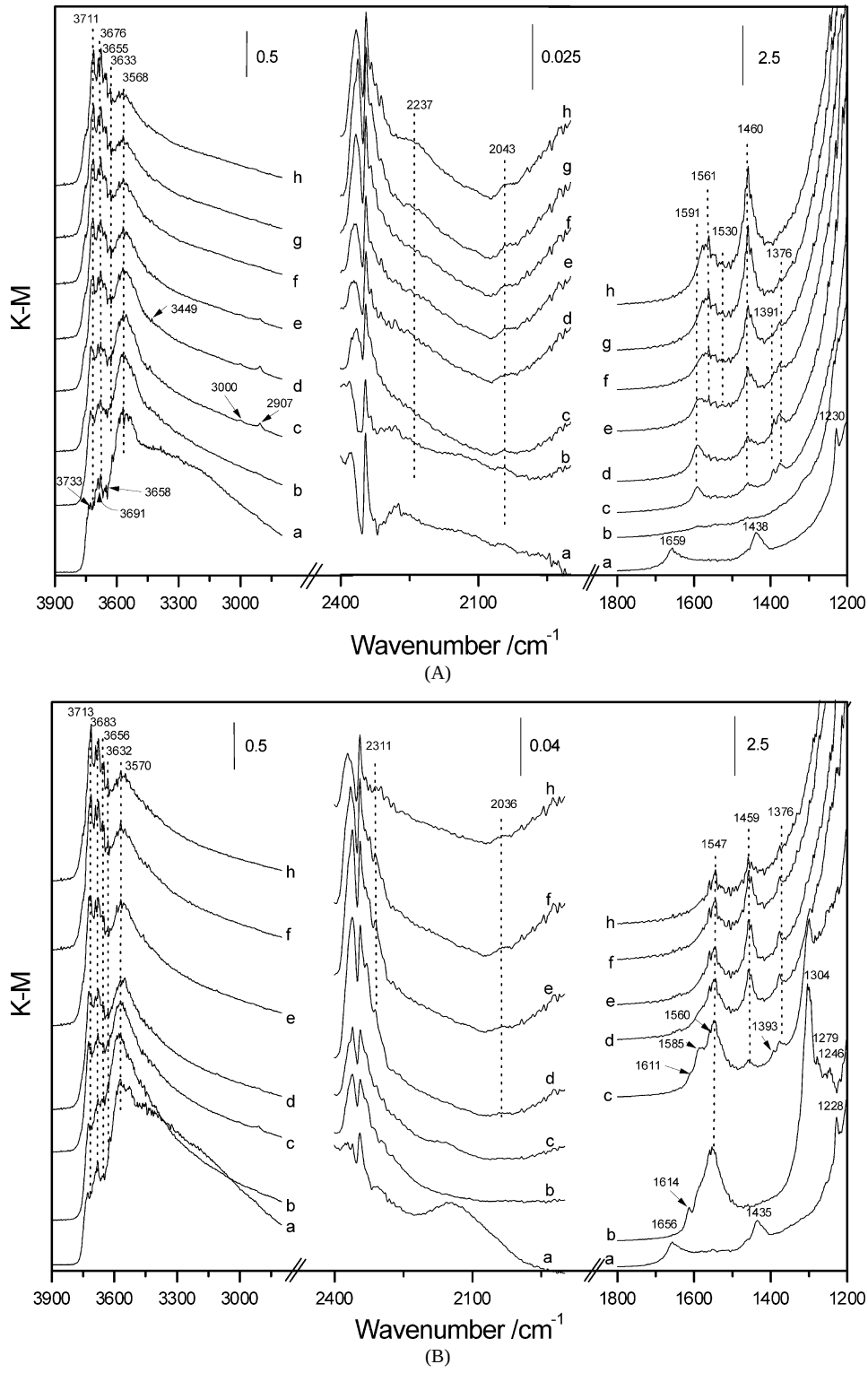

Fig. 6. DRIFTS spectra under reaction conditions for (A) alumina, (B) 1.5Ag, (C) 4.5Ag, and (D) 6Ag samples. Samples under dry air at 300 K (a) and under reaction conditions at 473 (b), 573 (c), 673 (d), 723 (e), 758 (f), 773 (g), and 798 K (h).

ably related to the nitrosonium (NO^+) species, which are possible (positively charged) intermediates in formation of nitrate species upon interaction of NO or NO_2 with surface hydroxyl or are concomitantly produced with nitrate-precursors molecules by disproportionation reaction of N-dimers [18,22,25,26]. On the other hand, the evolution of hydroxyl groups over the course of these experiments shows a strong dependence on the reaction temperature. Thus, whereas only limited consumption of basic hydroxyls and an accompanying increase of the more acidic groups is pro-

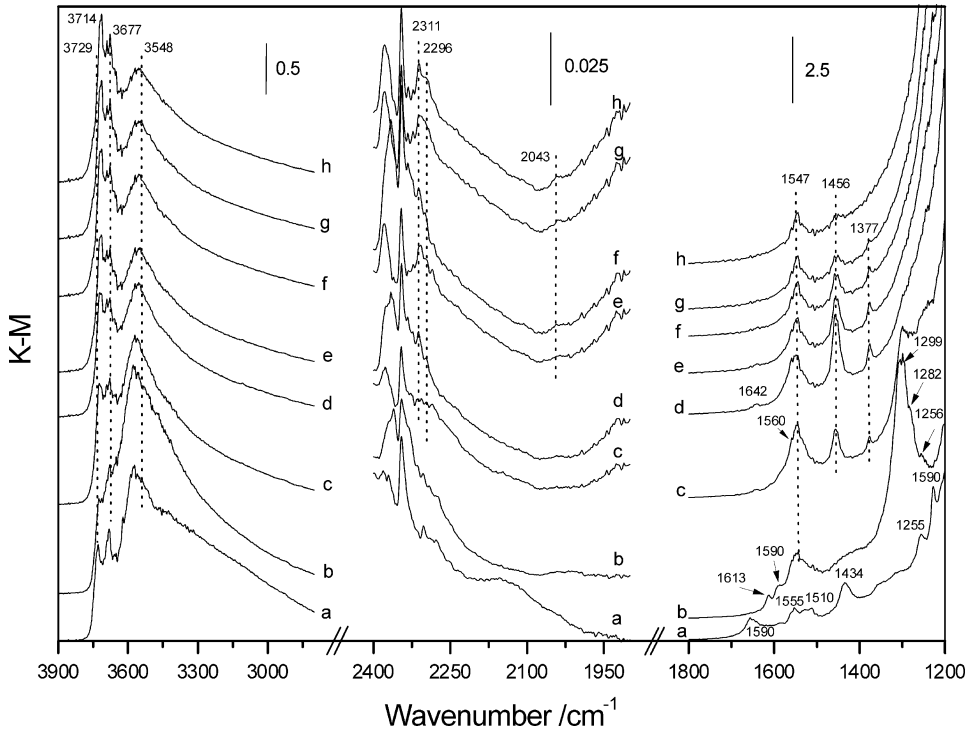

(C)

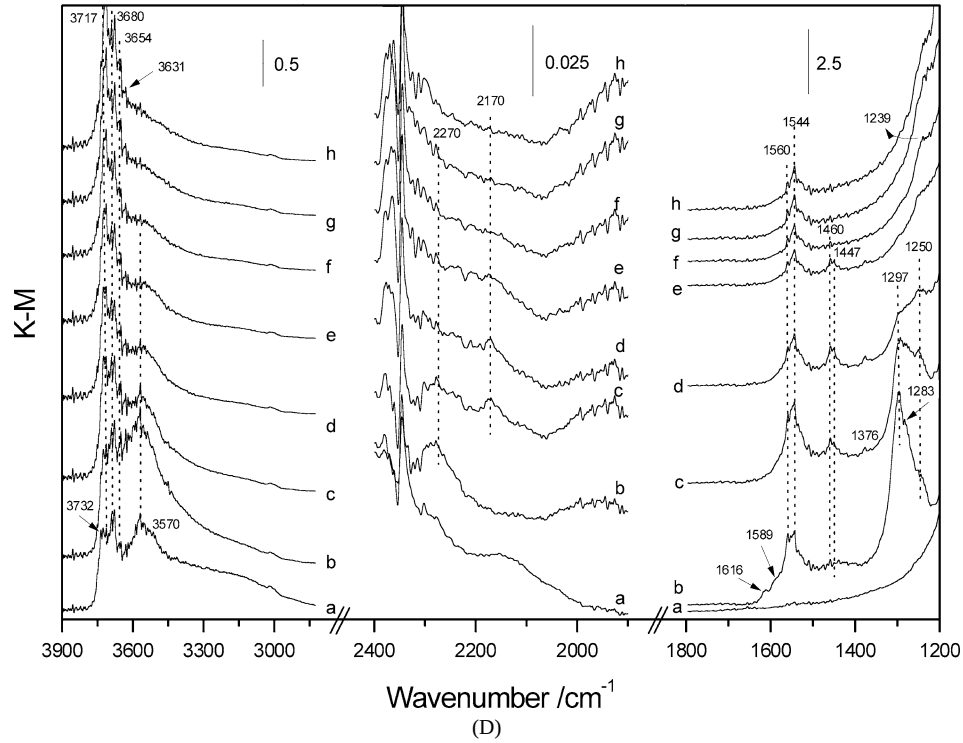

(D)

Fig. 6. Continued.

duced at low reaction temperatures (corresponding to relatively low conversion levels and in agreement with results displayed in Figs. 4 and 5), a more pronounced decrease of the latter is produced at higher reaction temperatures, and this is acute in the case of the 6Ag sample. As noted, production of water can concur in such phenomenon but seems not enough (band at ca. 1625 cm^{-1}) to justify the described changes in the hydroxyl region (Figs. 4–6).

3.4. In situ XAFS experiments

XANES and EXAFS spectra (Fig. 7 and 8, respectively) are shown for the most active catalysts (1.5Ag and 4.5Ag)

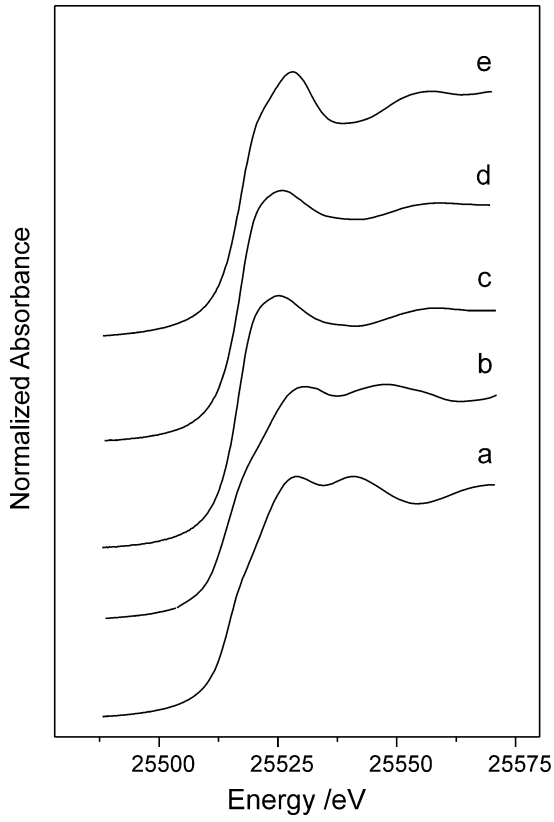

Fig. 7. XANES spectra of calcined Ag systems and reference materials: (a) Ag_2O, (b) α-$AgAlO_2$, (c) 1.5Ag, (d) 4.5Ag, and (e) β-$AgAlO_2$.

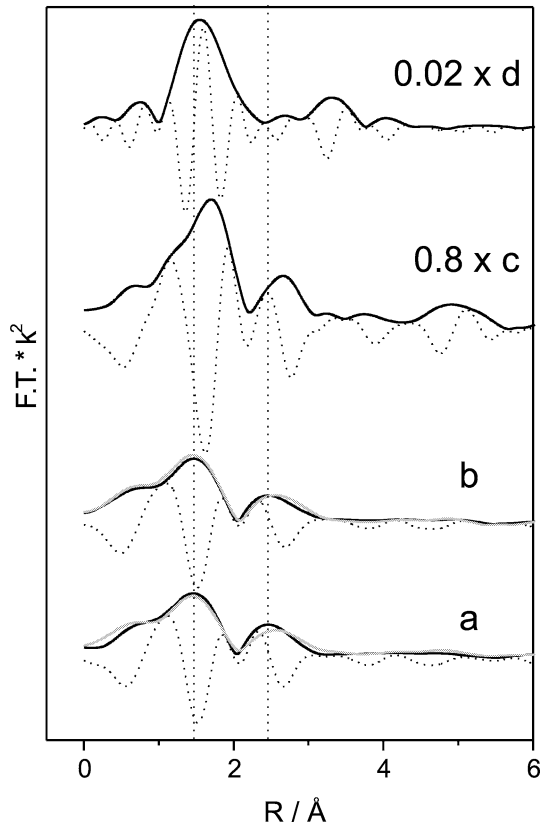

Fig. 8. FT of EXAFS spectra (1.95–8.2 $Å^{-1}$) for 1.5Ag and 4.5Ag samples and reference compounds: (a) 1.5Ag, (b) 4.5Ag, (c) β-$AgAlO_2$, and (d) Ag_2O. Black line, calcined materials; gray line, postreaction materials; full line, modulus; dashed line, imaginary part.

along with several reference compounds. The references (Fig. 7) may be classified in two groups, those which have a linear local silver geometry, as is the case for Ag_2O and α-$AgAlO_2$, and those with tetrahedral (or subgroup) symmetry β-$AgAlO_2$ [30]. The two active systems have XANES spectra which do not change under reaction conditions and display a high degree of similarity with the β-$AgAlO_2$ phase, giving strong support to an assignment of the active silver species to small silver aluminate particles but possessing tetrahedral symmetry. Small differences in intensity and in the position of continuum resonances (CRs) are a consequence of the small particle size of the aggregates and/or the interactions with the alumina support, as has been reported for many other supported-metal systems [31]. In fact, the shift to lower energy in the CRs at ca. 25525 eV, due to the 5sp electronic density, provides evidence that the Ag local coordination distances are modified with respect to the reference compound [31]. Further proof that the major part of silver is stable under reaction conditions is given in Fig. 8, where the Fourier Transform (FT) of EXAFS spectra of both systems is presented for samples measured in situ after calcination and after reaction at 773 K. From this figure it is clear that only a minimal part (less than 10%) of silver atoms undergo sintering. The comparison with the FTs of reference compounds displayed (Fig. 8) clearly indicates the presence of a contribution to the first Ag–O shell with shorter distance than those present in the β-$AgAlO_2$ phase. The Ag-cation distances which must contribute to the second peak of the FTs appear of a similar nature to those present in the β-$AgAlO_2$ reference and are located at shorter distances than the Ag–Ag contribution of the Ag_2O reference.

Analysis of the FTs presented in Fig. 8 gives evidence for three different Ag–O contributions, located at 2.15, 2.4, and 2.75 Å with coordination numbers of 0.30, 0.10, and 0.9 and Debye–Waller factors of 0.03, 0.015, and 0.065 $Å^2$, respectively, for 1.5Ag and 4.5Ag calcined materials (within a maximum deviation of ± 0.04 Å for the first and $\pm 15\%$ for the second and third parameters). The high disorder (probably non-Gaussian) displayed by the solids strongly limits the accuracy of the EXAFS fitting results. Moreover, they are additionally limited by the fact that both O anions and Ag/Al cations are expected as second nearest neighbors at distances close to 2.75 Å [30]. A correct fit may need to include Ag–Ag and Ag–Al contributions at the second coordination shell, a fact precluded by the absence of a confident Ag–Al phase and amplitude functions as well as for the limited number of fitting free parameters. In any case, the analysis performed is certainly indicative of the strong structural disorder at a local level displayed by the Ag samples.

Additional XANES experiments were performed to follow the reducibility of the Ag species present for the two

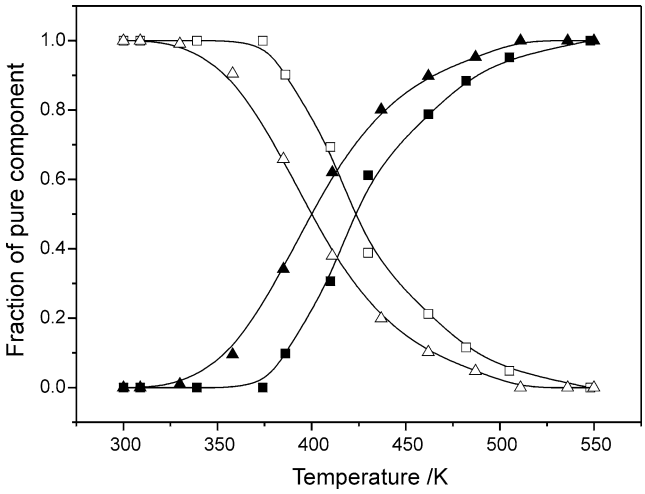

Fig. 9. Concentration profiles of silver species during a thermo-programmed run under 0.1% propene. Triangles, 4.5Ag; squares, 1.5Ag. Open symbols, initial, oxidized species; closed symbols, final, reduced species. See text for details.

most active catalysts. Analysis of data obtained during a temperature ramp in the presence of 0.1% propene using factor analysis [31] shows the presence of two silver-containing species, the initial beta silver aluminate and metallic silver at high temperature, with no clear differences between the 1.5Ag and 4.5Ag samples in terms of the shape of the corresponding XANES spectra. The important differences between the two samples concerns the onset temperature for reduction, indicated by the appearance of reduced silver species in Fig. 9, which is indicative of the enthalpy of formation of the oxygenated intermediates. Although this is unspecific for the different intermediates which may be formed, it indicates a more facile extraction of oxygen for the 4.5Ag sample, despite the similarity in the chemical nature of the Ag^+ species present initially in the calcined materials.

4. Discussion

The active silver species involved in the SCR of NO_x has been the subject of much debate although it is generally believed that highly dispersed Ag^+ cations are involved [5,15–20]. However, the local structure of such species which define the active phase has not been ascertained; it is only known that a strong interaction with the support is required to stabilize such species under reaction conditions and preclude the formation of zero-valent silver which favors the nonselective combustion of the hydrocarbon [5,15–20]. Comparison of the XANES shapes for the different samples (Fig. 8) and the Ag^+-containing reference compounds which may exist in the Ag/Al_2O_3 system clearly indicates that such cations possess (nearly) tetrahedral local coordination which closely resembles that of the β-$AgAlO_2$ reference. The EXAFS results suggest a significant local disorder around Ag centers as well as a noticeable reduction of the average Ag–O first shell coordination distance with respect to those present in the more regular, tetrahedral-like local structure of the β-$AgAlO_2$ material. Obviously, this local structure has notable differences with the linear structure typical of the Ag(I) oxide or alpha aluminate, which may be present in less active/selective systems. It is interesting to note that the linear, β-Al_2O_3-type $AgAl_{11}O_{17}$ aluminate has previously been detected in calcined alumina-supported silver samples [17]. This phase usually contains excess Ag cations between the characteristic alumina layers of the beta phase (which may be described as a $Ag(Ag_2O)Al_{11}O_{17}$ phase), and its catalytic performance may be poor as segregation of the Ag_2O entities with subsequent formation of Ag(0) particles could occur readily upon contact with a reducing agent (hydrocarbon) at reaction temperatures [16,17].

The stability of the species as indicated by the similarity of the XANES shape of the two active samples under reaction conditions, in agreement with UV–vis results (Fig. 2), indicates the absence of silver phase transformation processes, indicating a low probability for stabilization of other oxidation states (Ag(0) and AgO) or, as noted, of linear Ag^+ species during the course of the reaction. Additionally, the EXAFS results (Fig. 9) demonstrate that no significant particle size growth occurs under reaction up to 823 K. It is important to stress the absence of significant amounts of other silver redox states/phases, as this would hinder interpretation of DRIFTS results concerning the SCR mechanism and intermediates. Several TEM/EDS studies of Ag/Al_2O_3 systems in the 1–2 wt% range [5,17,18] have detected, particularly after reaction, the presence of large clusters of amorphous or poorly crystallized silver phases, which are very scarce in our micrographs and, as noted previously, do not influence the EXAFS spectra. Although the contribution of these aggregates to the exposed silver surface under reaction conditions may be argued, it is not clear if some of the intermediates and/or spectator species detected in previous studies may be associated with these phases.

In contrast to the behavior of the “low-loaded” samples, UV–vis results for the 6Ag sample (Fig. 2) indicate that changes in the nature of the silver species are produced in this sample during the course of the reaction. These can be related to the greater ease by which metallic silver states are generated in this sample, which would facilitate silver sintering processes above a certain temperature. In accordance with this hypothesis, formation of surface metallic silver states for this sample under reaction conditions is indicated by the ease by which NO dissociation takes place as inferred by the detection of adsorbed cyanide species at relatively low temperatures in the DRIFTS experiments (Fig. 6D). This is also in agreement with the formation of significant amounts of N_2O which is specific to this sample (Fig. 1), as NO dissociation/coupling reactive paths leading to N_2O formation can be related to the presence of metallic particles at the sample surface [32].

The mechanism of the NO-SCR with hydrocarbons has been extensively studied for silver [5,18,22,25,33,34], cobalt, and tin [9,35] on alumina samples, and a degree of similarity in terms of behavior and mechanism is apparent. It is generally accepted that both the hydrocarbon (propene) and NO molecules must first be activated by formation of some oxidized, adsorbed intermediates, typically carboxylates such as acrylate for the hydrocarbon and NO_2 or nitrite and nitrate compounds for NO [5,18,22,25,33–35]. Some of these activated, intermediate compounds may be present for the alumina support alone (Figs. 4 and 5), indicating that the support itself is, as well known, able to promote the SCR of NO_x using hydrocarbons as reducing agents. Silver is thought to play an important role in modifying the surface concentration and selectivity among these intermediates, enhancing the activity of the carrier. However, the coupling between these intermediates may occur primarily on the alumina surface and the role of silver in such coupling steps may be secondary [18,27,35]. It appears, therefore, that the main role of the metal may be restricted to the initial steps of the reaction and is mainly related to activation of the reactant molecules, either directly at the silver surface and/or by the modification of the acid/base (hydroxyls) properties of alumina (Fig. 3). DRIFTS results (Figs. 3–6) strongly support a clear role of active silver entities in modifying both the NO and the propene activation paths.

For NO, there is some evidence (Figs. 4 and 5), that NO may be activated by interaction with acidic hydroxyls, thus generating nitrosonium ion (NO^+) in a process involving H^+ (originating from the hydroxyls) consumption, as has been previously postulated for alumina [18] or zeolite-based systems [36,37]. Some of these NO-derived adsorbates are detected at high temperatures under reaction conditions (Figs. 6) and display maximum intensity for the most active (4.5Ag) sample. As observed in Fig. 4, such acidic hydroxyls are recovered by interaction with the hydrocarbon (or derived products), thus closing the catalytic cycle and regenerating the active surface species. Alternatively, nitrosonium ions plus nitrate precursor molecules (negatively charged N-containing molecules) can be simultaneously formed by disproportionation reaction of N-dimers (N_2O_3, N_2O_4) [25,37]. An additional pathway for nitrate formation is, as noted, reaction of NO_2(g) and hydroxyls groups. In any case, in our samples, two types of nitrates giving bands at ca. 1545–1550 and 1245 cm^{-1} (type I) and 1580–1590 and 1305 cm^{-1} (type II) are detected. Both measurements under reaction conditions during a light-off experiment (Fig. 6) and at low, steady-state conversion (Fig. 4) show the greater activity of type II nitrates. Type II nitrates are usually ascribed to bidentate species [22,25,26], which must therefore be considered as the NO-derived active entities which preferentially react with C-containing intermediates. Differences between the two active samples in this respect mainly concern the greater number of type II nitrates for 4.5Ag, but with no clear difference concerning the ratio of the N-containing ad-species was detected.

Hydrocarbon activation appears to be a very important step for silver systems [17,34] and, in fact, the reaction of an intermediate oxygenate hydrocarbon with the alumina surface is proposed as the rate-limiting step for supported tin catalysts [35]. Here, the hydrocarbon is activated in the presence of oxygen (Fig. 5, 6) initially at the methyl rather than the vinyl end of the molecule leading to a partial oxidation product with retention of the C=C bond and giving adsorbed acrylate. Oxidation via activation of the vinyl part of the molecule may give rise to the other carboxylate species, such as propanoate or ethanoate species. An alternative to the latter, concurrent scheme would be a consecutive route, where acrylate interacts with the appropriate acid–base centers of the alumina surface (consistent with modifications observed in the hydroxyl region of the infrared spectra in Figs. 3–5) and evolves in the presence of water with formation of acetaldehyde (plus formaldehyde) which, in turn, is subsequently attacked by NO-derived species after the rate-limiting step [35]. The proximity of surface Al sites (which act as anchoring sites for acrylate species) and Ag centers may be another reason for the high activity of the aluminate phase. As previously noted, consumption of surface hydroxyls is particularly significant for 6Ag, a fact which must influence N-activation (absence of type II nitrates) and should be considered, together with the presence of Ag(0) under reaction conditions, as a possible cause for the low selective reduction of propene with NO_x observed for this sample. On the other hand, formate, acetate, or other carboxylate-related compounds are fairly unreactive with either NO or O_2 alone but can be removed in $NO + O_2$ gas mixtures [16]. However, they do not seem to favor or have a negligible contribution to the coupling of N-species with the subsequent formation of N_2. DRIFTS results show that silver phases are involved in opening up alternative reaction pathways for hydrocarbon activation which lead to the generation of acrylate species, consistent with previous results from our laboratories [18]. Differences between the activities of the alumina alone and the supported silver samples are most likely related to some extent to the way in which the hydrocarbon is activated in each case which, as postulated in studies of partial oxidation of propene, can be related to the nature of the allyl intermediate formed in each case [26]. The silver-related phase may be involved in supplying the active oxygen species for the initial partial oxidation step and as shown in Fig. 9 the silver oxide anion species are in fact more labile for 4.5Ag than the 1.5Ag, which could then explain the higher NO_x reduction activity of the former (Fig. 1). This may favorably alter the rate of formation of the hydrocarbon intermediate. It can be noted, however, that the initial Ag–O distance and coordination numbers of our two active samples are very similar in the calcined state (as suggested by the EXAFS FTs displayed in Fig. 8) and only a very small variation after reaction is detected for the more active 4.5Ag sample. This small variation in size (and/or shape) could be the origin of the difference between the oxygen labilities detected for these two samples. Other parameters such as the number of active

sites for propene activation and or acrylate vs other types of carboxylate-related compound selectivity would appear to be of lesser importance. This comes from the fact that although the 4.5Ag system has a significantly greater number of silver sites for the activation of propene (IR intensity—Fig. 4), in the presence of NO this can be roughly balanced by the greater selectivity to acrylate species displayed by the 1.5Ag sample.

5. Conclusions

A series of Ag/Al_2O_3 catalysts with silver loadings in the 1.5–6 wt% range was prepared by an impregnation method employing EDTA complexes to promote a high dispersion of the silver phase. This was successful in obtaining highly active systems for silver loadings of 4.5 wt%. Structural analysis of the active silver phase gives evidence of a tetrahedral-like local symmetry for the active silver phase, with significant disorder and a Ag–O distance contribution to the first shell which is significantly shorter than the corresponding values for the symmetry-related (at a local level) β-$AgAlO_2$ phase. The high degree of stabilization of Ag(I) cations inserted into this structure contrasts with the more labile nature typically displayed by linear Ag species present either in oxide or aluminate phases [15–20].

The silver active species influences the reaction mechanism mainly by acting, in conjunction with alumina hydroxyls, in the activation steps of both NO and propene. For NO, positively charged N-containing ions and surface type II nitrates may evolve from N-containing dimers; the type II nitrate species being a potential intermediate which reacts with C-containing intermediates. Additionally, active silver species are involved in the opening of a route leading to adsorbed acrylate species as the active partially oxidized intermediate responsible for hydrocarbon activation. A possible relationship between the oxygen lability of the beta silver aluminate-like active phase and acrylate formation is postulated as being of importance in the catalytic performance of active silver systems.

Acknowledgments

A.I.-J. and A.B.H. thank the Comunidad Autónoma de Madrid for a predoctoral grant. Thanks are also due to the technical staff of BM29 line at ESRF Synchrotron for their hep during XAFS measurements. Dr. F. Del Monte for its kind support during the recording of UV–vis spectra. Support from CAYCIT (Project No. MAT 2000-1467) is greatly appreciated.

References

[1] M. Iwamoto, S. Yokoo, K. Saaki, S. Kagawa, J. Chem. Soc. Faraday Trans. 1 77 (1981) 1629.
[2] V.I. Parvulescu, P. Grange, B. Delmon, Catal. Today 46 (1998) 233.
[3] H.-W. Jen, Catal. Today 42 (1998) 37.
[4] T. Miyadera, K. Yoshida, Chem. Lett. (1993) 1483.
[5] T. Furisawa, K. Seshan, J.A. Lercher, L. Leffterts, K.-I. Aika, Appl. Catal. B 37 (2002) 205.
[6] R. Burch, P.J. Millington, A.P. Walker, Appl. Catal. B 4 (1994) 65.
[7] R. Burch, T.C. Watling, Appl. Catal. B 11 (1997) 207.
[8] T. Miyadera, Appl. Catal. B 2 (1993) 199.
[9] M.C. Kung, H.H. Kung, Topics Catal. 10 (2000) 21.
[10] S. Sumiya, M. Saito, H. He, Q.-C. Feng, N. Takezawa, K. Yoshida, Catal. Lett. 50 (1998) 87.
[11] T.N. Angelidis, N. Kruse, Appl. Catal. B 34 (2001) 201.
[12] F.C. Meunier, R. Ukropec, C. Stapleton, J.R.H. Ross, Appl. Catal. B 30 (2001) 163.
[13] A. Abe, N. Aoyama, S. Sumiya, N. Kakuta, K. Yoshida, Catal. Lett. 51 (1998) 5.
[14] T. Miyadera, Appl. Catal. B 16 (1998) 155.
[15] K.A. Bethke, H.H. Kung, J. Catal. 172 (1997) 93.
[16] K.-I. Shimizu, J. Shibata, H. Yoshida, A. Satsuma, T. Hattori, Appl. Catal. B 30 (2001) 151.
[17] N. Bogdanchikova, F.C. Meunier, M. Avalos-Borja, J.P. Breen, A. Prstryakov, Appl. Catal. B 36 (2002) 287.
[18] A. Martínez-Arias, M. Fernández-García, A. Iglesias-Juez, J.A. Anderson, J.C. Conesa, J. Soria, Appl. Catal. B 28 (2000) 29.
[19] T. Nakatsuji, R. Yasukawa, K. Tabata, K. Ueda, M. Niwa, Appl. Catal. B 17 (1998) 333.
[20] Z. Li, M. Flytzani-Stephanopoulos, Appl. Catal. A 165 (1997) 15.
[21] E.A. Stern, Phys. Rev. B 48 (1993) 9825.
[22] F.C. Meunier, J.P. Breen, V. Zuzaniuk, M. Olsson, J.R.H. Ross, J. Catal. 187 (1999) 93.
[23] T. Gerlach, U. Illgen, M. Bartoszek, M. Baerns, Appl. Catal. B 22 (1999) 269.
[24] (a) H. Knözinger, P. Ratnasamy, Catal. Rev. Sci. Eng. 17 (1978) 31;
(b) J.A. Anderson, C.H. Rochester, in: A. Hubbard (Ed.), Encyclopedia of Surface and Colloid Science, Dekker, New York, 2002, p. 2528.
[25] K. Hadjiivanov, Catal. Rev. Sci. Eng. 42 (2000) 71.
[26] A.A. Davydov, Infrared Spectroscopy of Adsorbed Species on the Surface of Transition Metal Oxides, Wiley, New York, 1984.
[27] V. Zuzaniuk, F.C. Meunier, J.R.H. Ross, J. Catal. 202 (2001) 340.
[28] K.-I. Shimizu, H. Kawabata, A. Satsuma, T. Hattori, J. Phys. Chem. B 103 (1999) 5240.
[29] G.M. Underwood, T.M. Miller, V.H. Grassian, J. Phys. Chem. A 103 (1999) 6184.
[30] W. Gessner, Z. Anorg. Allg. Chem. 352 (1967) 145.
[31] (a) M. Fernández-García, C. Márquez, G.L. Haller, J. Phys. Chem. 99 (1995) 12565;
(b) M. Fernández-García, Catal. Rev. Sci. Eng. 44 (2002) 59.
[32] M. Hirsimaki, M. Valden, J. Chem. Phys. 114 (2001) 2345.
[33] S. Sumiya, H. He, A. Abe, N. Takezawa, K. Yoshida, J. Chem. Soc., Faraday Trans. 94 (1998) 2217.
[34] K.-I. Shimizu, J. Shibata, A. Satsuma, T. Hattori, Phys. Chem. Chem. Phys. 3 (2001) 880.
[35] J.-H. Lee, A. Yezerets, M.C. Kung, H.H. Kung, Chem. Commun. (2001) 1404.
[36] T. Gerlach, F.-W. Schütze, M. Baerns, J. Catal. 185 (1999) 131.
[37] K. Hadjiivanov, J. Saussey, J.L. Freysz, J.C. Lavalley, Catal. Lett. 52 (1998) 103.